CORRELATIONS AND MEMORY IN NEURODYNAMICAL SYSTEMS

André Longtin[1], Carlo Laing[1], and Maurice J. Chacron[1]

University of Ottawa, Physics Department,
150 Louis Pasteur, Ottawa, Ont., Canada K1N 6N5

Abstract. The operation of the nervous system relies in great part on the firing activity of neurons. This activity exhibit significant fluctuations on a variety of time scales as well as a number of memory effects. We discuss examples of stochastic and memory effects that have arisen in our neuronal modeling work on a variety of systems. The time scales of these effects range from milliseconds to seconds. Our discussion focusses on 1) the effect of long-range correlated noise on signal detection in neurons, 2) the correlations and multistability produced by propagation delays, and 3) the long time scale "working memory" effects seen in cortex, and their interaction with intrinsic neuronal noise. We describe both analytical and numerical approaches. We further highlight the challenges of constraining theoretical analyses with experimental data, and of attributing functional significance to correlations produced by noise and memory effects.

1   Introduction

The study of the nonlinear dynamical properties of excitable systems poses great challenges. This is true from the single cell level all the way up to the macroscopic level of electric and magnetic fields recordings from large numbers of cells. The basic element of the nervous system is the nerve cell, or neuron, and its behavior is intrinsically nonlinear. Further, a single neuron is usually stimulated (or "forced", in the nonlinear dynamics context) by time-dependent signals of varying time scales and levels of stationarity, as well as by intrinsic noise sources related to the other neurons and to the intrinsic function of synapses and ionic conductances. The study of such stochastic nonlinear dynamics is at the forefront of research into nonlinear dynamics and how such dynamics are influenced by noise [26]. Further, in humans, there are on the order of 10^{10} nerve cells, and 10^{14} connections between them [27]. Basic groups of cells thought to perform a specific function, such as hypercolumns in the visual cortex usually contain thousands of cells. Yet even the study of two coupled neurons leads to a wealth of new phenomena not found at the single cell level, such as synchronization.

Neural modelers are well aware of this fact, and try to adapt the complexity of their models to the various phenomena they are interested in modeling, as well as to the available data. One common challenge is to decide whether or not to formulate the model in terms of Markovian dynamics such as ordinary differential equations, or in terms of non-Markovian models such as integro-differential models, or delay-differential equations which are a special case of them and arise often in the modeling of neural feedback. The modeler keen

to formulate nonlinear dynamical equations of motion for the assumed state variables of the system must also decide on whether or not to couple stochastic forces to deterministic models.

There are certainly philosophical issues underlying these choices. For example, one can argue that the evolution of the whole dynamical system of the brain relies only on the current state of all its components. And within this purview, activity in a given cell or group of cells may display correlations because it influenced the activity of another group of cells, which in turn later affect the behavior of the first group. In other words, due to the spatially distributed nature of the brain, activity recirculates in a more or less modified form. To avoid modeling the system as a whole, one may want to simplify using delayed dynamical systems; this allows one to dispose of spatial dimensions and concentrate on the time lag aspect of the recirculated activity [1,15,10]. Thus, non-Markovian dynamics result as a consequence of a modeling simplification. Another possibility is that by restraining a model to a certain number of state variables, the neglected ones which act on the system may do so in a non-stationary way, i.e. they cause non-stationary fluctuations on the time scale of the chosen state variables.

Given the complexity of excitable cell assemblies such as those in the nervous system of mammals, and even invertebrates, it is not surprising that long range correlations appear in recordings from these systems. Nevertheless, our level of understanding of the origin of these correlations is not well developed, and the functional implications of these correlations are even less clear. One certainly can think of many reasons why the nervous system should have long range correlations in its firing activity, such as for the storage and recall of significant experiences. The mechanisms governing this obvious potential use of long range correlations are beginning to be understood, and there is growing consensus that modifications of the strengths of connections between cells are implicated.

There are however many other kinds of nervous system activity that display correlations. For example, the firing of single cells in the auditory system, and other senses as well, have been shown to display long term correlations (see e.g. [47] for a review). Such correlations have been associated with various fractal noises, and it has been suggested that such noises arise through the normal functioning of the synaptic machinery that drives these cells. Also, as we mentioned above, the propagation of neural activity may be deemed slow in comparison to the time scale of the state variables of interest, or may not necessarily be slow, but has to propagate to other parts of the nervous system before influencing the dynamics of interest. Thus, delay-differential models are commonly seen, especially in the context of neural feedback and control [1,20].

Finally, it is known that nervous activity can be activated in a spatially specific manner, as occurs e.g. when we try to remember the spatial position where we saw a light appear for a second. The memory of this position is important e.g. if one wants to point to this position, either right away or after a minute. Thus, the activation of a spatially specific group of cells can be "remembered" by a spatially distributed model of the area of the brain involved in this so-called

"working memory" task. This memory will be either strengthened or decay away, and in any case influence the activity of the associated neurons on a long time scale. In this sense, it can be seen as a source of long range correlations. This memory will also be subjected to the effect of neuronal noise, which a priori would be considered as a limiting factor for the performance of this type of memory. We will report below on a paradoxical finding that suggests the opposite.

In this paper we present examples of neural dynamics that display long range correlations, and describe what is known about the functional implications for these correlations. We have a definite *bias towards nonlinear dynamical models*, rather than in developing more sophisticated techniques to characterize the correlations. In fact, the techniques discussed here to establish the presence and basic properties of the correlations are well-known. Further, the phenomena we have considered in our work operate at certain time and spatial scales, and do not include for example the important fields of ionic channel dynamics and neurohumoral dynamics (associated with the modulation of the concentration of various neurotransmitters and hormones on the time scale of seconds to days).

Our paper is organized as follows. In Section 2, we discuss the measurement, analysis and modeling of long range correlated firing in a class of neurons known as electroreceptors; the results are of general interest for all neurons. We further discuss how the correlations conspire to set up a time scale on which electrosensory system may best perform signal discrimination tasks. Section 3 considers the role of neural conduction delays in producing long range correlated activity, and briefly summarize what is known about the influence of noise on, and theoretical analysis of, noise in systems with delays. Correlations due to short term spatial memory, and their interaction with noise are the subject of Section 4. The paper is not meant to be comprehensive of long range correlated effects in neural systems. It does illustrate however how such correlation can arise in systems that range from the single cell level to the large scale spatial level. We have also arranged our presentation so that there is a progression from the small single cell spatial scale with "long range" correlations on the order of milliseconds, up to large spatial scales with longer range correlations on the order of seconds. In all examples, the correlations can be considered "long" because their time scale exceeds those of the dynamical components making up the systems.

2   Correlated Firing in Sensory Neurons

It is known that neural spike trains exhibit long range correlations [27,47] and there has been much speculation about their presence [47]. To this day, their functional role largely remains a mystery. However, many natural signals encoded by sensory neurons exhibit such long range correlations (e.g. music [49]). It has thus been speculated that long range correlations in neurons provides some advantages in terms of matching the detection system to the expected signal [46,47]. Many neural spike trains also exhibit short range correlations [36,42]. It has been shown that the spike train variability of these same neurons displays

a minimum as a function of the integration time. However, very little is known about how this can be generated in a biophysical neuron model.

Here we study how such a minimum can be generated in a simplified version of a model that has been used to model weakly electric fish electroreceptors [6–8]. The core of the model resides in the addition of threshold fatigue after an action potential to model refractory effects [19]. It is known that the model under Gaussian white noise stimulation gives rise to negative interspike interval (ISI) correlations that decay over short ranges [9]. We show that the addition of correlated noise gives rise to positive long range ISI correlations in the spike train generated by the model. These positive long range correlations lead to an increase in spike train variability at long time scales similar to that seen experimentally. They further interact with the short range negative ISI correlations to give rise to a minimum in spike train variability as observed experimentally. The functional consequences of both types of correlations is studied by considering their effects on the detectability of signals.

2.1 The Firing Model

A basic model for a neuron is the so-called integrate-and-fire model [27]: the neuron integrates its input in a leaky fashion (due to the RC properties of the membrane), and fires when the voltage reaches a firing threshold. After a firing, the voltage is reset to a value (such as zero) and the process repeats. *The reset destroys all memory of past firing events*, i.e. it makes the dynamics a "renewal process". Here we consider the following model modified integrate-and-fire model:

$$\frac{dv}{dt} = \Theta(t - T_{refrac})\left[-v/\tau_v + I + \xi(t) + \eta(t)\right] \quad \text{if } v(t) < s(t), \qquad (1a)$$

$$\frac{dw}{dt} = \frac{w_0 - w}{\tau_w} \quad \text{if } v(t) < w(t), \qquad (1b)$$

$$v(t^+) = 0 \quad \text{if } v(t) = w(t) \qquad (1c)$$

$$w(t^+) = w(t) + dw \quad \text{if } v(t) = w(t), \qquad (1d)$$

where v is the membrane voltage, w is the threshold, and I is the current. $\Theta(\cdot)$ is the Heaviside function ($\Theta(x) = 1$ if $x \geq 0$ and $\Theta(x) = 0$ otherwise). In between action potentials, the threshold w decays exponentially with time constant τ_w towards its equilibrium value w_0. We say that an action potential occurred at time t where $v(t) = w(t)$. Immediately after (i.e. at time t^+), we reset the voltage v to zero while we increment the threshold by a positive constant dw. The voltage v is kept equal to zero for the duration of the absolute refractory period T_{refrac}.

To model the intrinsic variability seen experimentally in neurons, we use two noise sources in the model (for details and justification see [7]): $\xi(t)$ is zero mean Gaussian white noise with variance D^2. $\eta(t)$ is zero mean Ornstein Uhlenbeck (OU) noise [18] with time constant τ_η and variance E^2. We take τ_η to be much larger than the intrinsic neural time scales (τ_v and τ_w).

Figure 1A illustrates the model dynamics. The noise sources $\xi(t)$ and $\eta(t)$ are shown in Fig. 1B. Note that we chose the noise source $\eta(t)$ to be two orders of magnitude weaker than the noise source $\xi(t)$. Also, $\xi(t)$ varies over short time scales while the noise $\eta(t)$ varies over longer time scales.

2.2   Interspike Interval Correlations

From the spike time sequence $\{t_i\}_{i=1}^N$, one can define the ISI sequence $\{I_i\}_{i=1}^n = \{t_{i+1} - t_i\}_{i=1}^{N-1}$. The ISI serial correlation coefficients (SCC) ϱ_j are a measure of linear correlations between successive ISIs. They are defined by

$$\varrho_j = \frac{< I_n I_{n+j} > - < I_n >^2}{< I_n^2 > - < I_n >^2} \ , \tag{2}$$

where $< \ . \ >$ denotes an average over the ISI sequence. The SCC ϱ_j is positive if the jth ISI and the current one are both (on average) shorter or longer than average. However, it is negative when the present ISI is shorter (longer) than average while the jth ISI is longer (shorter) than average.

Figure 2 shows the SCC sequence obtained with the model (black curve). One observes the presence of long range weak ISI correlations that decay exponentially with increasing lag. These are due to the presence of the OU noise $\eta(t)$ [7]. The SCC sequence obtained in the absence of Ornstein-Uhlenbeck noise (i.e. $E = 0$) does not show long range correlations (gray curve). The presence of long range correlations can be explained intuitively in the following manner [7]. The noise $\eta(t)$ varies on a slower time scale than the neural dynamics: it can thus be considered quasi-constant on the average ISI time scale. Thus, if the noise $\eta(t)$ is positive, it will stay positive for a long time (see figure 1B): this will lead to a long sequence of ISIs that will be shorter than average.

Note that in both cases (i.e. with and without OU noise), we have $\varrho_1 < 0$ (see inset). This is due to the deterministic properties of the model [9]. Figure 1A shows that if two spikes are fired during a relatively short time interval, there tends to be a summation effect in the threshold and it becomes higher than average. Consequently, the next ISI will tend to be long since the threshold takes a longer time to decay. A similar argument holds if two spikes are separated by a long time interval. Thus short ISIs will tend to be followed by long ISIs and vice versa, and this will give rise to $\varrho_1 < 0$. This property can be studied by looking at the model's deterministic response to perturbations [9].

We now explore the consequences of these short and long range ISI correlations on spike train variability. We denote by $p(n, T)$ the probability distribution of the number of action potentials obtained during a counting time T. $p(n, T)$ is referred to as the spike count distribution [3,45]. The Fano factor [14] measures the spike train variability on multiple time scales. It is defined by

$$F(T) = \frac{\sigma^2(T)}{\mu(T)} \ , \tag{3}$$

where $\mu(T)$ and $\sigma^2(T)$ are the respective mean and variance of $p(n,T)$. The asymptotic value of the Fano factor is related to the SCC sequence [11]

$$F(\infty) = CV^2 \left(1 + 2\sum_{i=1}^{\infty} \varrho_i \right), \tag{4}$$

where CV is the coefficient of variation: it is given by the ratio of the standard deviation to the mean of the ISI distribution.

We plot the resulting Fano factor curves (Fano factor versus counting time) for the model in Fig. 3A. The Fano factor curve obtained in the absence of OU noise (triangles) decreases monotonically. However, the presence of the weak OU noise affects the spike train variability at long time scales by increasing the Fano factor (squares). Due to the finite correlation time of the OU process, the Fano factor saturates to a finite value. We now explain the phenomenon in more detail. Let us assume the following form for the SCC's with $i > 1$:

$$\varrho_i = -0.34355\delta_{1i} + 0.007\exp(-i/347.768), \tag{5}$$

where δ_{ij} is the Kronecker-delta ($\delta_{ij} = 1$ if $i = j$ and 0 otherwise). This was obtained by an exponential fit of the data in Fig. 2 with OU noise as well as adding the value of ϱ_1. Substituting (5) into (4) yields an asymptotic expression (upper black horizontal line) for the Fano factor that is close to that observed numerically. This justifies our assumptions about exponentially decaying ISI correlations.

We compare the results with the Fano factor obtained from the randomly shuffled ISI sequence; the shuffling eliminates all ISI correlations and a renewal process results (circles). The Fano factor $F(T)$ now decreases monotonically towards the asymptotic value given by CV^2 ("CV^2" line in Fig. 3A). This is in accordance with (4). We observe that the presence of short term negative ISI correlations decreases spike train variability at long time scales. However, weak long range ISI correlations will give an increase in spike train variability at long time scales. This is consistent with the predictions from (4).

Figure 3B shows the corresponding mean (open squares) and variances of the spike count distribution obtained under all three conditions. It is observed that the reduction in the Fano factor caused by negative ISI correlations is primarily due to the fact that the variance is reduced at long time scales in comparison with a renewal process (compare filled circles and open triangles). The noise $\eta(t)$ is too weak to have any noticeable effect on the mean. However, it significantly increases the variance of the spike count distribution at long time scales (filled squares).

It is thus an interaction between negative and positive ISI correlation coefficients that gives rise to the minimum in the Fano factor curve. This minimum counting time depends upon the strength E and time constant τ_η of the OU process [7]: it is possible to change the counting time at which the minimum occurs by changing the parameter E [7]. Furthermore, the counting time at which the saturation occurs depends on τ_η: the saturation point can be set to arbitrarily large counting times by increasing τ_η.

2.3 Detection of Weak Signals

We now discuss the use of signal detection theory [21] to assess the consequences of ISI correlations on the detectability of signals. This is based on the optimal discrimination of spike count distributions in the absence and presence of a stimulus ($P_0(n, T)$ and $P_1(n, T)$, respectively). Let us suppose that the firing rate is f_0 in the absence of stimulus and that it is f_1 in the presence of a stimulus. If the stimulus is weak and excitatory, it will give an increase in the mean of the spike count distribution without significantly increasing the variance [42,7]. Thus, we assume $\sigma_0^2(T) = \sigma_1^2(T)$ and $\mu_1(T) = (f_1/f_0)\mu_0(T)$. One can then quantify the discriminability between $P_0(n, T)$ and $P_1(n, T)$ by [21]

$$d' = \frac{\mu_0(T)|f_1/f_0 - 1|}{\sqrt{2}\,\sigma_0(T)}\ . \tag{6}$$

The situation is illustrated in Fig. 4A. The discriminability d' is inversely related to the amount of overlap between the distributions $P_0(n, T)$ and $P_1(n, T)$. To quantify the changes in d' caused by both types of ISI correlations, we form the difference between d' obtained from the ISI sequence with ISI correlations and the d' obtained for the corresponding renewal process (i.e. the shuffled ISI sequence); we will use the symbol $\Delta d'$ to denote this difference. Figure 4B shows the measure $\Delta d'$ as a function of counting time T. A maximum can be seen around $T = 200$. Note that this corresponds to the counting time at which the Fano factor $F(T)$ is minimal. Thus, the improvement in signal detectability is maximal when spike train variability (as measured by the Fano factor) is minimal.

2.4 Discussion of Correlated Firing

We have shown that a simple model with correlated noise can give rise to both short and long range ISI correlations. The dynamic threshold could model synaptic plasticity [16], recurrent inhibition [13], or intrinsic ionic conductances that lead to adaptation [32]. The effects discussed here can thus originate from very different physiological and biophysical mechanisms. Deterministic properties of the model have been shown to lead to negative interspike interval correlations at short lags. These negative ISI correlations lead to lower spike train variability at intermediate time scales: they thus regularize the spike train at long time scales.

It was further shown that the addition of a very weak noise with long range correlations could induce exponentially decaying long range positive ISI correlations in the model. These positive ISI correlations were shown to lead to increased spike train variability at long time scales. This increase in spike train variability at long time scales has been observed in many neural spike trains [47,27]. It has been observed that synaptic vesicle release rates display long range correlations [37] and our OU process $\eta(t)$ could model these fluctuations. The noise $\xi(t)$ could then model fluctuations occurring on very short time scales such as channel and/or synaptic noise.

We have shown that both short range negative and long range positive ISI correlations interact to give a minimum in spike train variability at an intermediate counting time. This minimum has been observed experimentally in auditory fibers [36] as well as in weakly electric fish electroreceptors [42]. We have previously reproduced this effect using a detailed electroreceptor model [7]. However, the present study shows that similar effects can be obtained in a simple model with dynamic threshold and correlated noise. The functional consequences of this minimal counting time were assessed using signal detection theory. It was shown that the model under Gaussian white noise stimulation displayed only short range negative ISI correlations [6,9]. That result was reproduced here. It was further shown that negative ISI correlations reduced spike train variability as measured by the Fano factor at long time scales.

Using signal detection theory, we have shown that the improvement in signal detectability was maximal, as compared to a renewal process, when the Fano factor was minimal. It has been shown in weakly electric fish electroreceptors that the counting time at which the Fano factor is minimal corresponds to the behavioral time scale for prey detection [39]. Animals must make decisions in short amounts of time (usually less than a second) in order to survive (i.e. to detect prey or avoid predators). Thus, the presence of short term negative ISI correlations might serve to increase signal detectability while long term positive ISI correlations will give rise to an integration time at which spike train variability is minimal. It could be that the animal does not want to integrate the signal over longer time scales for which the spike train variability increases again.

3   Delayed Neurodynamical Systems

We now turn to the role of delays in inducing long range correlations. Even though we focus on neural systems, given our past work on such systems, the ideas we will be discussing are sufficiently general to be applicable to many other areas where delays are important such as laser physics and economics. We will discuss how delayed dynamics arise, and focus on how they generate correlations that outlast the delay (which is the intrinsic memory of the system) and on how to approach their analysis in the presence of noise, which is of particular importance in the nervous system [27].

3.1   Delay-differential Equations

We focus on correlations in delay-differential equations (DDEs) of the general form

$$\frac{dx}{dt} = f\left(x(t), x(t - \tau), \boldsymbol{\mu}, \xi(t)\right) . \tag{7}$$

We will restrict ourselves to such first order delay equations, and in particular, to those having only one delay. We will also discuss specific instances of this equation in the context of neuronal modeling, statistical physics of bistable systems and atmospheric physics. The DDE (7) can be seen as a dynamical system that

combines aspects of ordinary differential equations (ODEs) and discrete time maps. This equation can also be seen as a special case of the integro-differential system

$$\frac{dx}{dt} = f(z(t), \boldsymbol{\mu}) \tag{8}$$

with

$$z(t) = \int_{-\infty}^{t} K(t - s) x(s) \, ds \,. \tag{9}$$

In this more general case, the kernel $K(t)$ weighs the past values of $x(t)$ that influence the dynamics of dx/dt in the present. If the function f is linear, the problem is completely solvable, e.g. using Laplace transforms. The solutions are of the same types as for any other linear ordinary differential equation. However, note that since a DDE is an infinite-dimensional dynamical system, even though there appears to be only one dynamical variable, the class of equations above can exhibit oscillatory solutions, which are not possible in one-dimensional ODEs. For the linear case, such solutions are either continually growing or decaying in amplitude, or are marginally stable (pure imaginary eigenvalues).

Below we focus on discrete delays. However, it is important to realize that in most situations, the delay is actually distributed. In laser cavities, it is a good approximation to make the delay fixed, as it corresponds to the travel time of light around some optical path. DDEs are also an approximation to the whole dynamics governing propagation of effects in various media. For example, in physiology, delays are often introduced to take the maturation time of cell populations into account simply, rather than having extra compartments (and associated dynamical equations) for the maturation process. Likewise in neural systems, delays represent propagation times along axons, as well as synaptic delays. A description of such processes in terms of delays avoids the complexities of partial differential equations for the propagation of action potentials along the nerve, and extra ordinary differential equations associated with synaptic activation and release processes.

It is important to include delays in the description of a physical process when it is of a magnitude comparable to or larger than the other time scales found in the system. For example, if the relaxation of a system to its steady state is dominated by a time scale τ_{sys}, then it is important to take into account any delays on the order of or larger than τ_{sys}.

3.2   Correlations

Delays induce correlations. This can be simply understood by considering the time evolution of the dynamical system: $x(t + dt)$ depends on $x(t)$ and on $x(t - \tau)$. For example, if for the current value of $x(t)$, the derivative $f(x(t), x(t - \tau))$ is positive, $x(t)$ will increase. Since $x(t - \tau)$ influences the sign of f, there can be a positive or negative correlation between $x(t)$ and $x(t - \tau)$. The linear correlation between these two quantities can be measured using the standard autocorrelation function $\langle x(t) x(t - \tau) \rangle$. If the solution is chaotic, it will typically

display peaks at multiples of the delay, superimposed on an overall decaying background [38]. Such structure will also be seen if noise is incorporated into the dynamical equations, leading to a "stochastic delay-differential system" (SDDE) in the latter case. Of course, the peaks will be repeated periodically, along with all the rest of the autocorrelation function, if the solution is periodic.

Usually, there is sufficient knowledge about the system under study to conclude the presence of delays. However, sometimes that fact is not clear, or the value of the delay is not known, or there could be more than one delay. There exist time series methods that allow the detection of delays, as well as estimation of these delays [25].

3.3   Delayed Neural Control

Delays arise often in the context of neural control, such as in the control of light flux on the retina in the pupil light reflex (PLR). This reflex is in fact a paradigm of neural control systems [44]. This system is interesting from an experimental point of view because it can be manipulated non-invasively using infrared video-pupillometry coupled with special light stimulation. In past work on the human pupil light reflex [33], we have been able to study the onset of oscillations as the gain of this control system is artificially increased. We have been quickly confronted with noisy fluctuations in the analysis and modeling of this system. This is not surprising given that this reflex naturally exhibits ongoing fluctuations ("hippus") in healthy humans under constant light stimulation. Such baseline fluctuations are in fact common in neural and physiological control, and their origin and meaning is a subject of great interest and debate [20]. They just happen to be especially prominent in the light reflex. The origin of these fluctuations there is still elusive, but our modeling using a first order DDE strongly suggests that they are the manifestation of neuronal noise injected into the reflex arc. The delayed negative feedback dynamics of this system can be simply modeled by

$$\frac{dA}{dt} = -\alpha A(t) + f(A(t - \tau)) = -\alpha A(t) + C\frac{\theta^n}{\theta^n + A^n(t - \tau)} + K, \qquad (10)$$

where A is the pupil area. A supercritical Hopf bifurcation occurs as the parameter n, controlling the slope of the feedback function (i.e. the feedback gain), or the fixed delay τ, are increased. This model correctly predicts the oscillation frequency, as well as the slow variation and robustness of this frequency across the bifurcation. It does not exhibit other bifurcations as the gain is increased from zero (open-loop) or as τ is increased at fixed gain. Also, the fact that hippus occurs in open-loop signifies that its origin is not deterministic chaos arising from the nonlinear delayed feedback, as seen for example in the Mackey-Glass equation [20]. The noisy oscillations may then arise because neural noise perturbs the dynamics of the PLR. This hypothesis has been tested by introducing noise on K (additive noise) or on C (multiplicative noise) in (10). The questions we are ultimately seeking to answer are, is it noise, and if so, what is the

origin of this noise, its spectrum before entering the reflex arc, and its coupling to the reflex arc? Any progress along this line would be of great interest given that the pupil reflects brainstem function as well as higher brain function such as attention and wakefulness, and any better discrimination of the associated states using non-invasive monitoring of the pupil size can yield important new diagnostics.

We do not have the space to provide details about our analysis here. In summary, we have found by numerical integration of (10) that pupil area fluctuations can arise from the coupling of the PLR to colored neural noise of Ornstein-Uhlenbeck type with a correlation time of one second. This fact is based on the ability of the model to reproduce key features of the time series (beyond the frequency), such as the behavior, as a function of gain, of the mean and variance of the period and amplitude of the fluctuations [33]. Thus the hypothesis of feedback dynamics coupled to noise as in (10) seems very appropriate. The experimental data are insufficient however to establish the proportions of additive and multiplicative noise. Also, the analysis highlights the difficulty of pinpointing the gain value at which the Hopf bifurcation occurs. The problem is that oscillations are always visible due to the noise, even when the system should exhibit a fixed point if the noise were not present. The power spectra of area time series do not exhibit critical behavior. In fact, the behavior of this system at a Hopf bifurcation under the influence of noise does not differ from that of nonlinear stochastic ODEs near such a bifurcation.

The usual way around this problem of pinpointing a bifurcation when noise is present is to devise an order parameter which does exhibit critical behavior, and that can be calculated theoretically. An order parameter that has been proposed for a noisy Hopf bifurcation [26,33] is based on the invariant density of the state variable. The order parameter is the distance between the two peaks of this density, i.e. it measures its bimodality. The density is unimodal on the fixed point side, and bimodal on the limit cycle side, with the peaks roughly corresponding to the mean maximal and minimal amplitude of a stochastic oscillation. The behavior of this parameter can be compared between simulations, theory (stationary density of the Fokker-Planck equation) and actual measured data.

Unfortunately, Fokker-Planck analysis is not possible for DDEs such as (10), because they are non-Markovian. Furthermore, such an approach requires many data points to resolve the peaks, and thus compute the order parameter, especially in the vicinity of the deterministic bifurcation. Thus the approach is limited for physiological data. However, numerics reveal the interesting fact that noisy oscillations look qualitatively similar to the data as a function of the gain. Simulations also reveal the fact that additive or multiplicative noise on (10) actually move the onset of the bifurcation point towards the limit cycle side [33,34]. From the point of view of the order parameter, there is a "postponement" of the Hopf bifurcation in the first order DDE (10) (see the general discussion of such effects in [26]). From the time series point of view, even though the order parameter is still zero, the time series is clearly oscillatory, with the mean oscillation

amplitude increasing with the gain parameter, while the frequency varies little across the stochastic bifurcation.

Even though it is not possible to compute the invariant density for (10) due to the delay, its solutions are useful to validate hypotheses about noise. One can, for example, compute various statistics about the noisy oscillations and compare them between model and data. This approach allows us to state that additive or multiplicative lowpass Gaussian noise injected in the pupil light reflex can explain the results seen as the gain is varied. This approach is interesting because it allows one to put the noise under the magnifying glass, given that noise dominates the behavior of systems in the vicinity of bifurcations where the usual dominant linear terms are weak or vanish. What the approach does not give is the origin of this noise, although it can be used to test for some of its properties, such as its variance and possibly higher order moments, and what its correlation structure is. In fact, the best results occurred in our comparative study when the noise had a correlation time on the order of 300 msec (lowpass filtered Gaussian white noise, i.e. Ornstein Uhlenbeck noise, was used). Better data would allow to better pinpoint the correlation time, which in turn can give more insight about its origin. For example, it could be fast synaptic noise, slow retinal adaptation noise, or slow neural discharge activity from the reticular activating system that governs wakefulness and which is injected in the PLR at the brainstem level.

There have been recent efforts at analyzing noise in DDEs, and the field is wide open and rife with potential Ph.D. projects. We have done a systematic study of stochastic DDEs in the low noise limit using Taylor expansions of the flow, and indicated the limits of validity of this approach [22]. The Taylor expansions allow one to use the Fokker-Planck formalism. The agreement between analytical approximations and the numerical simulations are good for small delays. However, the agreement decreases when the underlying dynamics are oscillatory; in particular, this arises when the characteristic equation that arises from the linearization around a fixed point has complex eigenvalues. The Taylor expansions of first order DDEs can only produce first order ODEs, which can not have complex eigenvalues, thus the limitation of this approach.

The noise-induced transitions between the two wells of a delayed bistable system have also been investigated following the same formalism and show the same quality of agreement and intrinsic limitations [23]. That delayed dynamical system reads

$$\frac{dx}{dt} = x(t - \tau) - x^3(t - \tau) + \xi(t) , \qquad (11)$$

where $\xi(t)$ is Gaussian white noise. There has also been recent work by Ohira [40] that approximates this DDE by a special random walk. From this walk, approximations to the stationary density, correlation functions and even an approximate Fokker-Planck equation have been obtained. There has also been work applying the ideas of two-time scale perturbation theory to stochastic DDEs [28]. Finally, a master equation in which the transition rates are delay-dependent has been recently proposed [48] for a stochastic DDE which is the standard quartic system

(particle in a bistable potential) with linear additive feedback and noise

$$\frac{dx}{dt} = x(t) - x^3(t) + \alpha x(t - \tau) + \xi(t) =; ,$$ (12)

where α is a constant. In [48], the authors actually solve only for the case where $x(t-\tau)$ is replaced by its sign, thereby losing information on the precise dynamics within the wells. However, this formalism is very promising as it allows the computation of the mean switching time between the wells as a function of the delay τ and the feedback strength α. It is left to be seen how well the formalism works for a wider range of parameters, since we have recently shown that the deterministic dynamics of (12) are rather complex, and involve a Takens-Bogdanov bifurcation [43]. It should be mentioned that this equation is of special interest in the atmospheric physics literature as well, where it has been used as a toy model of the El Niño Southern Oscillation phenomenon (see a discussion of this in [43] and references therein). Another interesting study of a stochastic delay equation in the context of neurology with comparison to experiments can be found in [10].

Finally, let us mention two other aspects where delays and noise are bound to be increasingly under scrutiny in the future. One has to do with neural dynamics at the single neuron level, and involves delays of a few milliseconds. When a neuron fires at its soma, the effect is propagated to other neurons it is connected to, but also to the dendritic tree of the neuron. Depending on the ionic channels in this tree, the spike may propagate back down, influencing and even causing further spiking at the soma. This can lead to temporally correlated sequences of spikes, such as bursting patterns [12]. The modeling of such phenomenon is complex, given the spatio-temporal nature of the problem in complex geometry, resulting in partial differential equations that must be solved numerically. However, we have recently shown that the resulting correlation and memory effects on the millisecond time scale that occur in such backpropagation of action potentials from the soma to the dendrites can be modeled with a DDE [31]. We suspect that such dynamics, in combination with noise, can yield long range correlations as well. Also, systems in which the delay is larger than the system response time can often exhibit multistability, i.e. coexistence of deterministic attractors, each with their own basin of attraction. This implies that two different initial functions may yield different steady state behaviors [2]. Further, noise will kick the trajectories from one attractor to another, which may also produce long range correlations. A discussion of this multistability in the neural context can be found in [15].

4   Noise Induced Stabilization of Bumps

4.1   Background

There has been much recent interest in spatially-localized regions of active neurons ("bumps") as models for feature selectivity in the visual system [4,5] and

working memory [24,29,50], among others. Working memory involves the holding and processing of information on the time scale of seconds. For these models, which involve one-dimensional arrays of neurons, the position of a bump is thought to encode some relevant aspect of the computational task. Simple versions of these models do reproduce the basic experimental aspects of short term memory [24,29].

One problem, however, is that more realistic models of the neurons involve what are known as adaptation effects. Spike frequency adaptation, in which the firing frequency of a neuron slowly declines when it is subject to a constant stimulus, is ubiquitous in cortical neurons [32]. It is known that including such adaptation in a general model for bump formation destabilizes stationary bumps, causing moving bumps to be stable instead [30]. This was shown in [30], for a particular model, to be due to a supercritical pitchfork bifurcation in bump speed as the strength of adaptation was increased. The bifurcation occurred for a non-zero value of adaptation strength. The implication of this destabilization is that, while the bump may initially be at the position that codes for the spatial stimulus, the movement of the bump will destroy this information, thus degraded the performance of the working memory.

It was also shown in [30] that adding spatiotemporal noise to a network capable of sustaining bumps effectively negated the effect of the adaptation, "restabilizing" the bump. This beneficial aspect of noise is similar in spirit to stochastic resonance [17], in which a moderate amount of noise causes a system to behave in an optimal manner. We now demonstrate this phenomenon, and later summarize its analysis.

4.2   Stochastic Working Memory

The system we study is a network of integrate and fire neurons, in which each neuron is coupled to all other neurons, but with strengths that depend on the distance between neurons. The equations for the network are

$$\frac{dV_i}{dt} = I_i - a_i - V_i + \frac{1}{N}\sum_{j,m} J_{ij}\alpha(t - t_j^m) - \sum_l \delta(t - t_i^l) \tag{13a}$$

$$\tau_a \frac{da_i}{dt} = A\sum_l \delta(t - t_i^l) - a_i \, , \tag{13b}$$

for $i = 1, \ldots, N$, where the subscript i indexes the neurons, t_j^m is the mth firing time of the jth neuron. $\delta(\cdot)$ is the Dirac delta function, used to reset the V_i and increment the a_i. The sums over m and l extend over the entire firing history of the network, and the sum over j extends over the whole network. The postsynaptic current is represented by $\alpha(t) = \beta e^{-\beta t}$ for $0 < t$ and zero otherwise. The variable a_i, representing the adaptation current, is incremented by an amount A/τ_a at each firing time of neuron i, and exponentially decays back to zero with time constant τ_a otherwise. The coupling function we use is

$$J_{ij} = 5.4\sqrt{\frac{28}{\pi}}\exp\left[-28\left(\frac{i-j}{N}\right)^2\right] - 5\sqrt{\frac{20}{\pi}}\exp\left[-20\left(\frac{i-j}{N}\right)^2\right] \, . \tag{14}$$

This is a "Mexican hat" type of coupling, for which nearby neurons excite one another, but more distant neurons inhibit one another. Periodic boundary conditions are used. Parameters used are $\tau_a = 5$, $\beta = 0.5$, $N = 50$, $A = 0.1$. I_i was set to 0.95 for all i, except for a brief stimulus to initiate a bump, as explained in the caption of Fig. 5. When $I_i = 0.95$ for all i, the quiescent state, $(V_i, a_i) = (0.95, 0)$ for all i, is a solution. However, it is known that with coupling of the form (14), and $A = 0$, stationary patterns of localized activity are also possible solutions [29,30].

Noise was included in (13a)-(13b) by adding or subtracting (with equal probability) current pulses of the form σe^{-t} $(0 < t)$ to each otherwise constant current I_i. The arrival times of these pulses were chosen from a Poisson distribution. The mean frequency of arrival for both positive and negative pulses was 0.1 per time unit, so the frequency for all pulses was 0.2 per time unit. The arrival times were uncorrelated between neurons. The noise intensity was varied by changing σ.

In Fig. 5 we show typical simulation results for (13a)-(13b) for two different noise levels. A spatially localized current was injected for a short period of time $(10 < t < 20)$ to move the system from the "all off" state to a bump state. This could mimic e.g. the briefly illuminated light in an oculomotor delayed response task [24,41]. We see that the activity persists after the stimulus has been removed. This is a model of the high activity seen during the "remembering" phase of a working memory task [41].

The behavior of the system for the two different values of noise is quite different: for low noise values, the bump moves with an almost constant speed. For the example in Fig. 5 (left), the bump moves to the right. This is due to the lack of symmetry in the initial conditions – it could have just as easily traveled to the left. Note that the boundary conditions are periodic. For higher noise intensities (Fig. 5, right) the bump does not have a constant instantaneous speed, rather it moves in a random fashion, often changing direction. As a result of this, the average speed during a finite-time simulation (determined by measuring how far the bump has traveled during this time interval and dividing that distance by the length of the interval) is markedly less than in the low noise case.

This is quantified in Fig. 6 where we plot the absolute value of the average speed during an interval of 200 time units (not including the transient stimulus phase) as a function of σ, averaged over eight simulations. We see that there is a critical value of σ (approximately 0.01) above which the absolute value of the velocity drops significantly – this is the "noise-induced stabilization".

4.3   Discussion of Noisy Bumps

The phenomenon discussed above is quite robust with respect to changes in parameters, and has also been observed in a rate model description of bump formation, in which the individual action potentials of each neuron have been temporally averaged so that each neuron is only described by its instantaneous firing rate [30]. Noise-induced stabilization was analyzed in some detail in [30], and we now briefly summarize the results.

As mentioned, the phenomenon was also observed in a spatially-extended rate model. For a particular choice of the coupling function (the spatially continuous version of J_{ij} (14)) it was shown that the bifurcation destabilizing a stationary bump and giving rise to traveling bumps was a supercritical pitchfork bifurcation in bump speed as A increased. Motivated by this, the noisy normal form of such a bifurcation was studied and (when velocity was measured in the same way as for the spiking neuron model above) qualitatively similar slowing down was found as the noise intensity was increased.

Motivated by these results we modeled the dynamics of the noisy normal form of a supercritical pitchfork bifurcation as a persistent random walk in one dimension. The behavior of a particle undergoing such a walk is governed by the stochastic differential equation

$$\frac{dx}{dt} = I(t) \; , \tag{15}$$

where x is the position of the particle (the bump), $I(t) \in \{-v, v\}$, and the probability that $I(t)$ changes from $-v$ to v, or from v to $-v$, in time interval dt is $(\beta/2)dt$. The probability density function of x, $p(x, t)$, satisfies the telegrapher's equation:

$$\frac{\partial^2 p}{\partial t^2} + \beta \frac{\partial p}{\partial t} = v^2 \frac{\partial^2 p}{\partial x^2} \; . \tag{16}$$

This equation can be explicitly solved, and the mean absolute position at time t, and the variance of this quantity, can both be found analytically [30]. They are

$$\langle |x(t)| \rangle = vte^{-\beta t/2}[I_1(\beta t/2) + I_0(\beta t/2)] \tag{17}$$

and

$$\langle |x(t)|^2 \rangle = 2v^2(\beta t - 1 + e^{-\beta t})/\beta^2 \; , \tag{18}$$

where the angled brackets denote averaging over realizations, and $I_{0,1}$ are modified Bessel functions of the first kind of order $0, 1$. Once we link β to noise intensity via an Arrhenius-type rate expression, e.g. $\beta = e^{-1/\sigma}$, we can use (17) and (18) to generate a plot like Fig. 6 – see Fig. 7. This agrees qualitatively with the results of the simulations of the full spiking network, (13a)-(13b), and provides an explanation for the phenomenon of noise-induced stabilization.

5 Conclusion

We have presented an overview of various ways in which long range correlations can arise in neurodynamical systems. These range from the millisecond time scale to time scales of many seconds in our work. There are of course much longer time scales (relating e.g. to behavior) on which correlations can be seen, and which are related to changes in the level of expression of various receptors and hormonal concentrations. This is beyond the scope of our own research. Rather we have focussed on how noise can induce short and long range correlations in single cell firing activity, and the potential importance of this effect

for information coding. Also, we have considered how correlations arise from the delays in the propagation of neural activity, with particular attention paid to the effect of external fluctuations on such processes, and on bifurcations to oscillatory behavior in particular. Finally, we have considered how localized "bumps" of activity arise in realistic neural nets. These are thought to underlie short term memory processes, and the ongoing formation and movement of these bumps will result in correlated firing in single or multi-electrode recordings. Our analysis of such phenomenon with noise has enabled us to reduce a complex spatiotemporal problem to a simple first order differential equation with noise, an approach that may prove useful in other contexts where patterns of activity in excitable systems are under study.

There are still a large number of open problems in these areas, as we have alluded to in the discussion of the three main sections of our paper. Multistability and memory (non-renewability) in first passage time problems, as well as the analysis of noise in PDEs for excitable system, will in our view offer theorists and numerical analysts some of the most challenging problems for decades to come, and their study will certainly forward our understanding of the nervous system.

References

1. U. an der Heiden: J. Math. Biol. **8**, 345 (1979).
2. F.T. Arecchi, A. Politi and L. Ulivi: Il Nuovo Cimento, **71**, 119 (1982).
3. H.B. Barlow HB, W.R. Levick WR: J. Physiol. (Lond) **200**, 11 (1969).
4. R. Ben-Yishai, R. L. Bar-Or and H. Sompolinsky: Proc. Natl. Acad. Sci. USA. **92**, 3844 (1995).
5. P. C. Bressloff, N. W. Bressloff and J. D. Cowan: Neural Comp. **12**, 2473 (2000).
6. M.J. Chacron, A. Longtin, M. St-Hilaire, L. Maler: Phys. Rev. Lett. **85**, 1576 (2000).
7. M.J. Chacron, A. Longtin, L. Maler: J. Neurosci.**21**, 5328 (2001).
8. M.J. Chacron, A. Longtin, L. Maler: Neurocomputing **38**, 129 (2001).
9. M.J. Chacron, K. Pakdaman, A. Longtin: Neural Comput. (2002) (in press).
10. Y. Chen, M. Ding and J.A.S. Kelso, Phys. Rev. Lett. **79**, 4501 (1997).
11. D.R. Cox, P.A.W. Lewis: *The statistical analysis of series of events* (Methuen, London, 1966).
12. B. Doiron, C.R. Laing, A. Longtin and L. Maler: J. Comput. Neurosci. **12**, 5 (2002).
13. B. Ermentrout, M. Pascal, B. Gutkin: Neural Comp., **13**, 1285 (2001).
14. U. Fano: Physiol. Rev. **72**, 26 (1947).
15. J. Foss, A. Longtin, B. Mensour and J.G. Milton: Phys. Rev. Lett. **76**, 708 (1996).
16. G. Fuhrmann, I. Segev, H. Markram, M. Tsodyks: J. Neurophysiol., **87**, 140 (2002).
17. L. Gammaitoni, P. Hänggi, P. Jung and F. Marchesoni: Rev. Mod. Phys. **70**, 223 (1998).
18. C.W. Gardiner: *Handbook of stochastic methods* (Springer, Berlin, 1985).
19. C.D. Geisler, J.M. Goldberg: Biophys. J., **6**, 53 (1966).
20. L. Glass and M.C. Mackey: *From Clocks to Chaos. The Rhythms of Life.* (Princeton U. Press, 1988).
21. D. Green, J. Swets: *Signal Detection Theory and Psychophysics* (Wiley, New York, 1966).

22. S. Guillouzic, I. L'Heureux and A. Longtin: Phys. Rev. E **59**, 3970 (1999).
23. S. Guillouzic, I. L'Heureux and A. Longtin: Phys. Rev. E **61**, 4906 (2000).
24. B. S. Gutkin, C. R. Laing, C. L. Colby, C. C. Chow and G. B. Ermentrout: J. Comput. Neurosci. **11**, 121 (2001).
25. R. Hegger, M.J. Bunner, H. Kantz and A. Giaquinta: Phys. Rev. Lett. **81**, 558 (1998).
26. W. Horsthemke and R. Lefever: *Noise-Induced Transitions. Theory and Applications in Physics, Chemistry and Biology*. (Springer Verlag, New York, 1984).
27. C. Koch: *Biophysics of Computation*, (Oxford UP, New York 1999).
28. R. Kuske, preprint (2002).
29. C. R. Laing and C. C. Chow: Neural Comput. **13** (7), 1473 (2001).
30. C. R. Laing and A. Longtin: Physica D **160**, 149 (2001).
31. C. R. Laing and A. Longtin: Bull. Math. Biol. (2002) (in press).
32. Y.-H. Liu and X.-J. Wang: J. Comput. Neurosci. **10**, 25 (2001).
33. A. Longtin, J.G. Milton, J. Bos and M.C. Mackey: Phys. Rev. A **41**, 6992 (1990).
34. A. Longtin: Phys. Rev. A **44**, 4801 (1991).
35. A. Longtin and J.G. Milton: Math. Biosc. **90**, 183 (1988).
36. S.B. Lowen, M.C. Teich: J. Acoust. Soc. Am. **92**, 803 (1992).
37. S.B. Lowen, S.S. Cash, M. Poo, M.C. Teich: J. Neurosci. **17**, 5666 (1997).
38. B. Mensour and A. Longtin: Physica D **113**, 1 (1998).
39. M.E. Nelson, M.A. MacIver: J. Exp. Biol. **202**, 1195 (1999).
40. T. Ohira: Phys. Rev. E. **55**, R1255 (1997).
41. S. G. Rao, G. V. Williams and P. S. Goldman-Rakic: J. Neurophysiol **81**, 1903 (1999).
42. R. Ratnam, M.E. Nelson: J. Neurosci. **20**, 6672 (2000).
43. B. Redmond, V.G. LeBlanc and A. Longtin: Physica D (2002) (in press).
44. L. Stark: *Neurological Control Systems: Studies in Bioengineering*. (Plenum, New York, 1969).
45. M.C. Teich, S.M. Khanna SM: J. Acoust. Soc. Am. **77**, 1110 (1985).
46. M.C. Teich: IEEE Trans. Biomed. Eng. **36**, 150 (1989).
47. M.C. Teich: 'Fractal neuronal firing patterns'. In: *Single neuron computation*. ed. by T. McKenna, J. Davis, S.F. Zornetzer (Academic, San Diego 1992) pp. 589-622.
48. L.S. Tsimring and A. Pikovsky: Phys. Rev. Lett. **87**, 250602 (2001).
49. R.F. Voss, J. Clarke: J. Acoust. Soc. Am. **63**, 258 (1978).
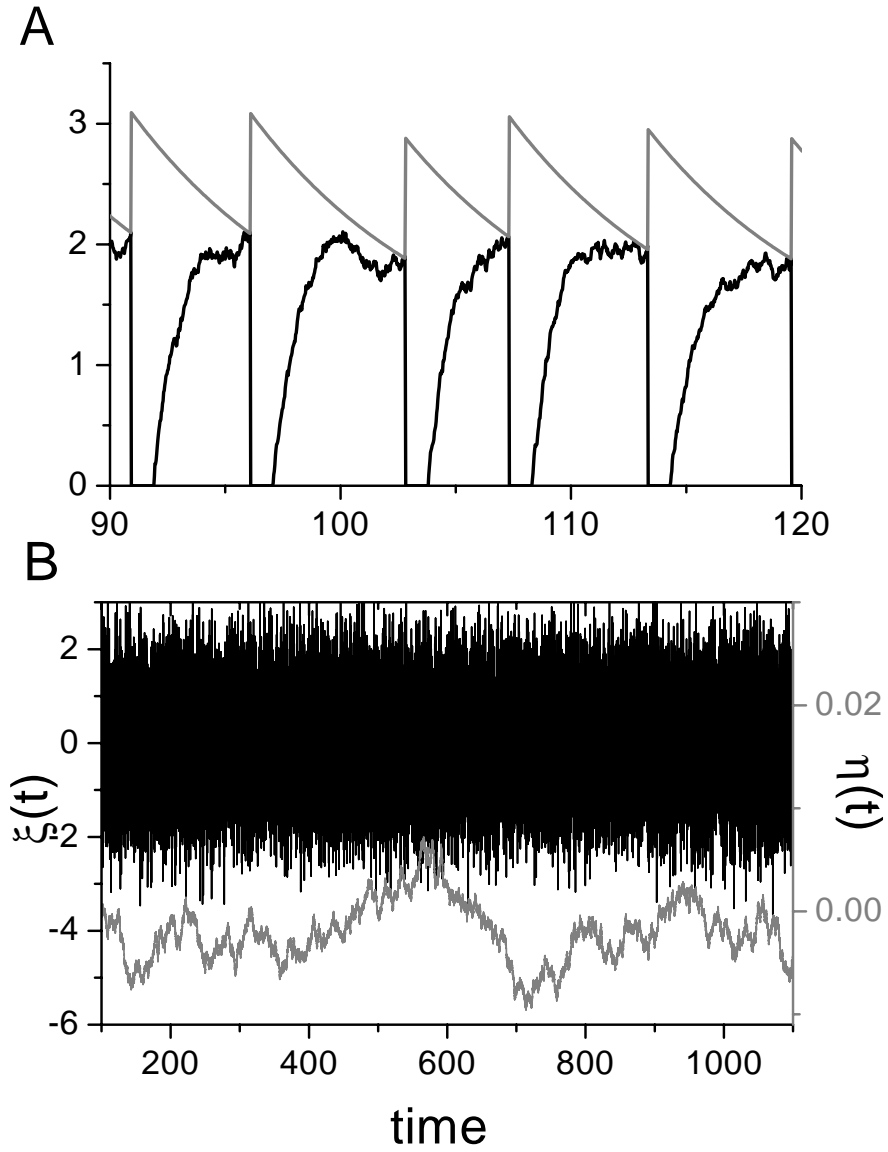50. X.J. Wang: J. Neuroscience **19**, 9587 (1999).

Fig. 1. (**A**) voltage (*black solid line*) and threshold (*gray solid line*) time series obtained with the model. (**B**): The noise sources obtained with the model: $\xi(t)$ (*upper black solid line*) is two orders of magnitude greater than $\eta(t)$ (*lower grey solid line*). Parameter values are: $\tau_v = 1, \tau_w = 8.63, I = 2, T_{refrac} = 1, \tau_\eta = 2000, D = 0.95, E = 0.00306$
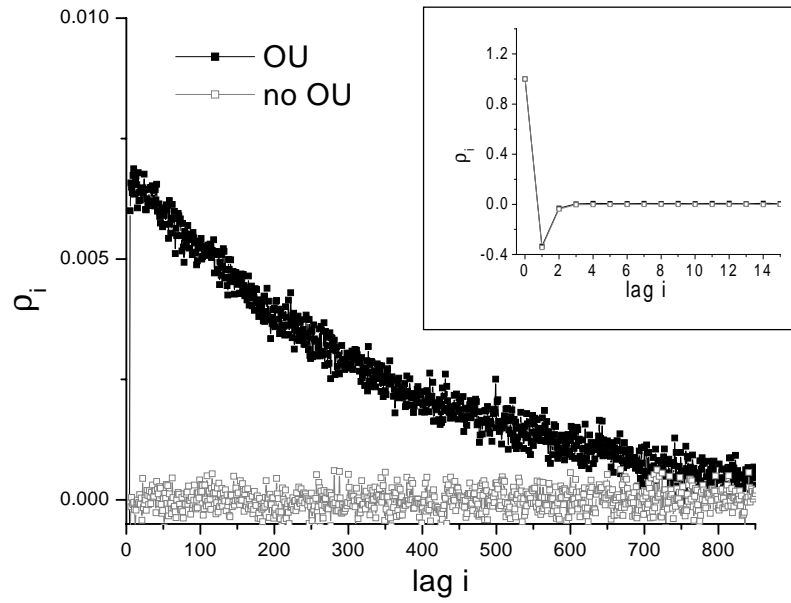
Fig. 2. The ISI correlation coefficients obtained from the model with (*black*) and without (*grey*) OU noise. Weak positive ISI correlations that decay exponentially are present with OU noise but are not without. However, both cases show the presence of a negative SCC at lag one (inset). It was necessary to generate 10^7 action potentials to reveal the presence of the weak positive ISI correlations
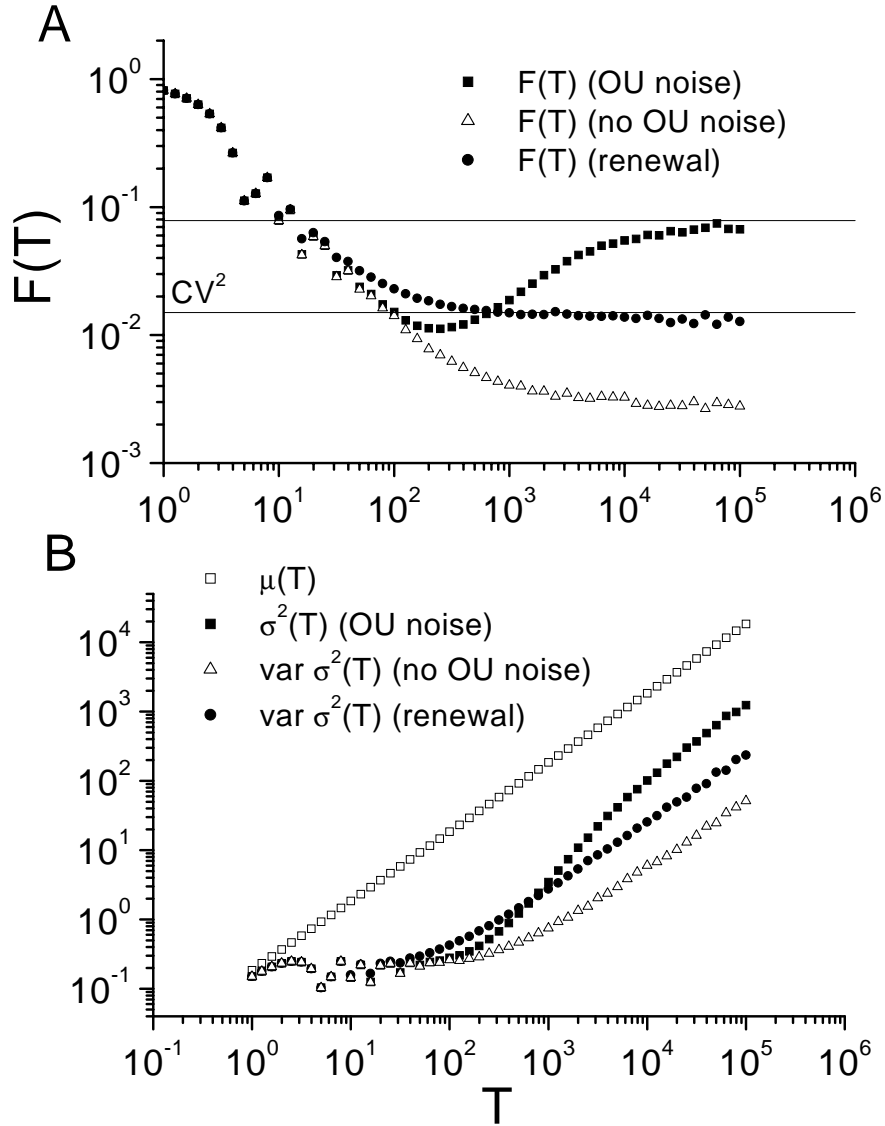
Fig. 3. (**A**) Fano factor obtained with (*filled squares*), and without (*open triangles*) OU noise. Also plotted is the Fano factor obtained without any ISI correlations (*filled circles*). (**B**) The mean (*open squares*) and variance of the spike count distribution obtained with (*filled squares*) and without (*open triangles*) OU noise. Also shown is the variance obtained without any ISI correlations (*filled circles*)
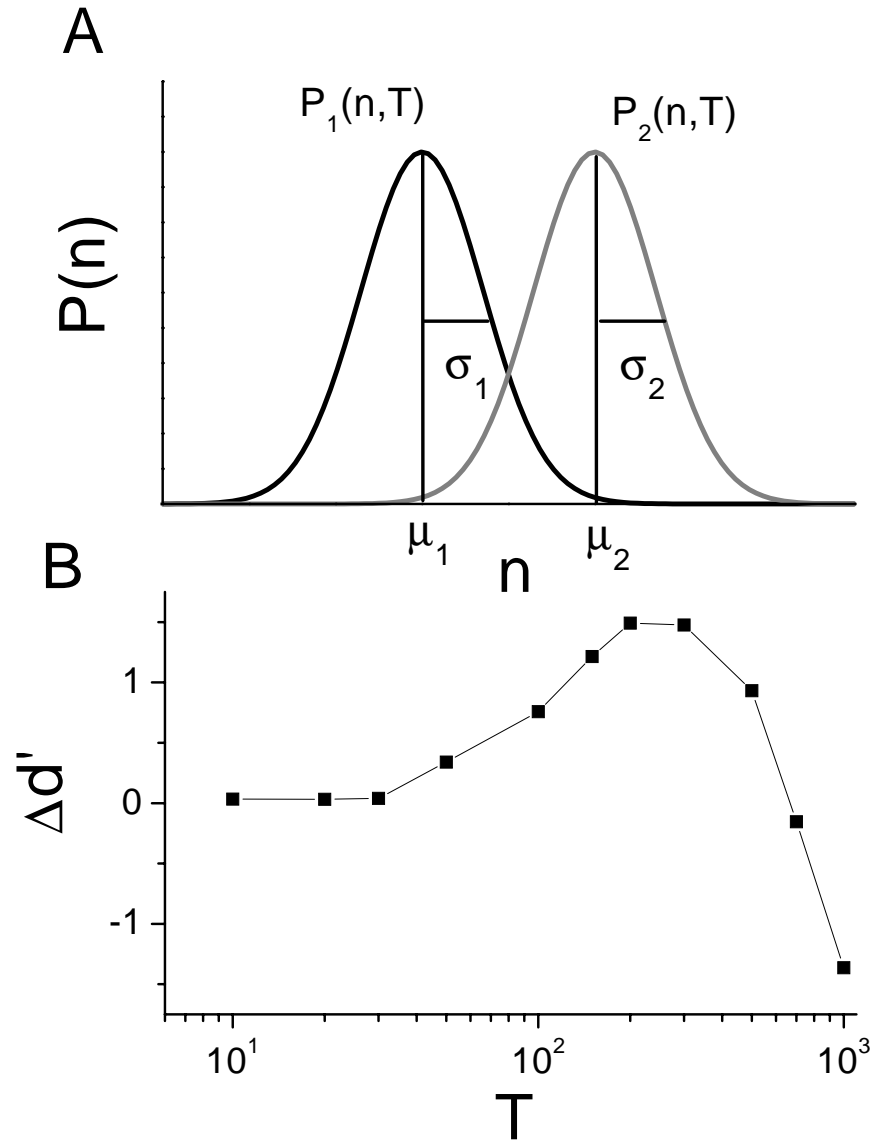
A

B

Fig. 4. (**A**) The spike count distributions $P_0(n,T)$ and $P_1(n,T)$ along with their respective means and variances. (**B**) Difference between the d' measure obtained with OU noise and the d' measure obtained with a renewal process $\Delta d'$ as a function of counting time T. A optimal counting time at which signal detectability is maximal is seen. We took $f_1 = 215Hz$ and f_0 was equal to the mean firing rate of the neuron in the absence of stimulus
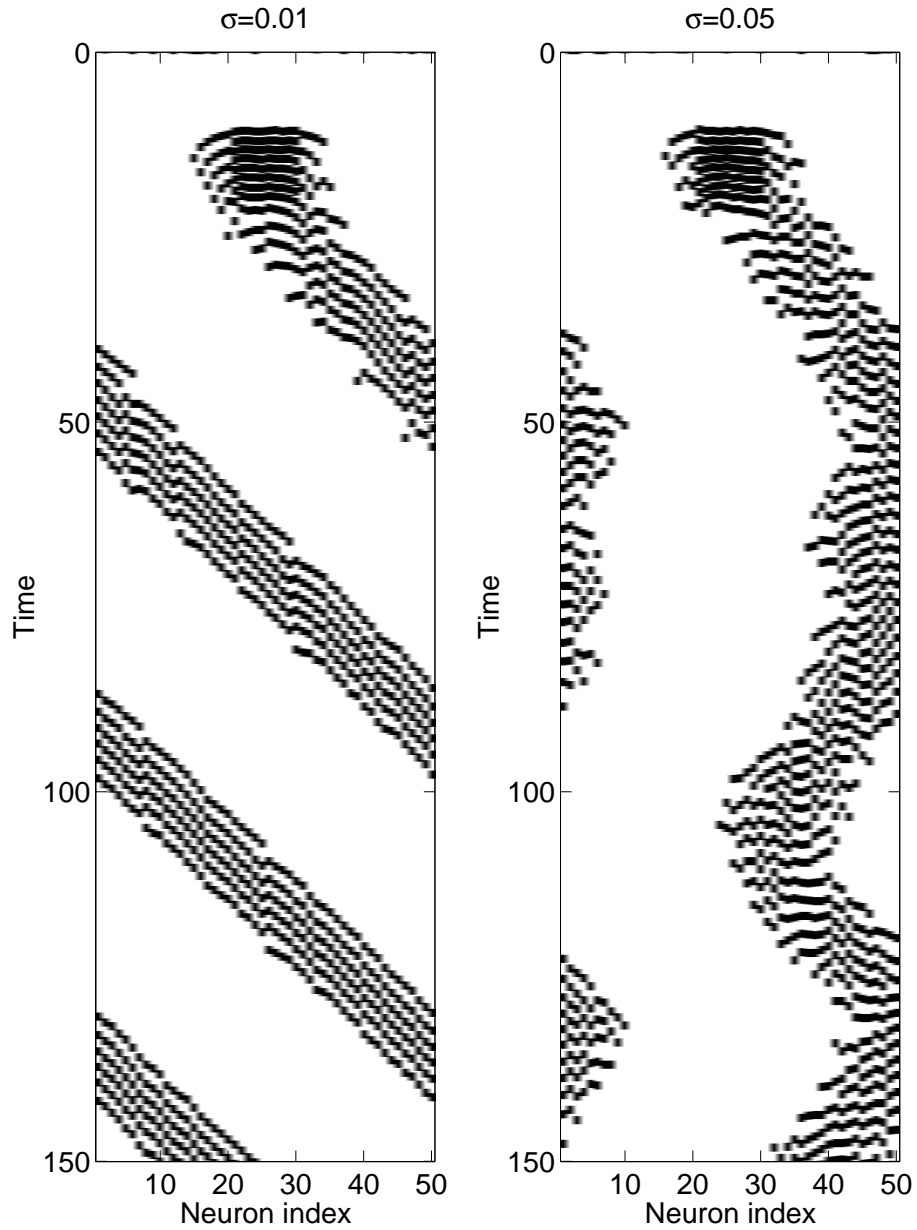
Fig. 5. Typical simulations of (13a)-(13b). (**Left**) $\sigma = 0.01$, (**Right**) $\sigma = 0.05$. A black bar is plotted each time a neuron fires (its voltage reaches 1). I was set to 1.2 for neurons 21 to 30 for $10 < t < 20$, otherwise it was set to 0.95. Other parameters are given in the text. The boundary conditions are periodic.
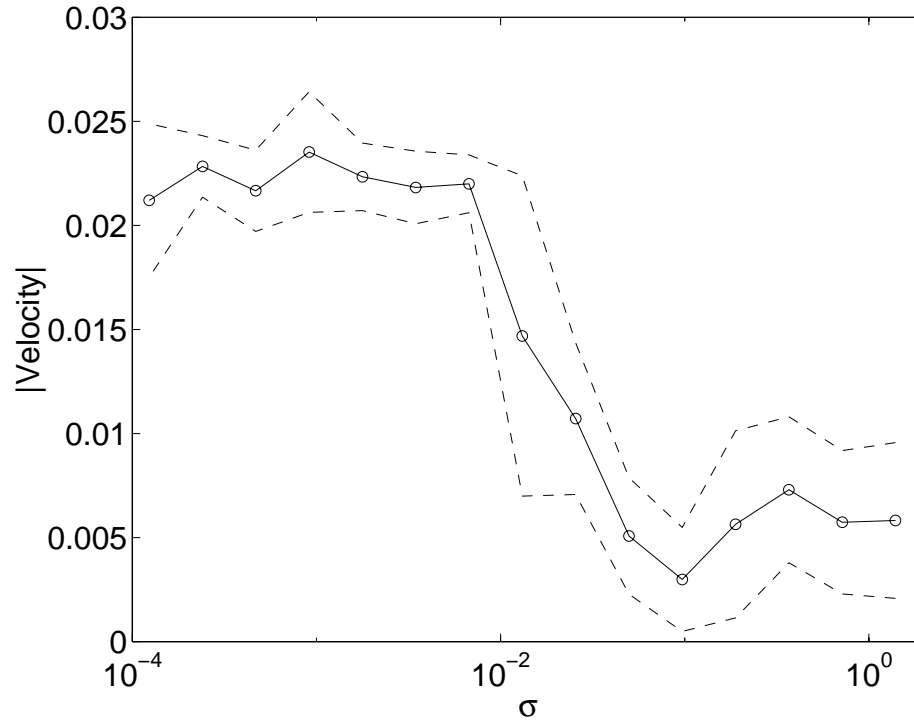
Fig. 6. Absolute value of the velocity of a bump for (13a)-(13b) during a period of 200 time units, as a function of noise intensity σ. The *dashed lines* indicate plus and minus one standard deviation about the mean
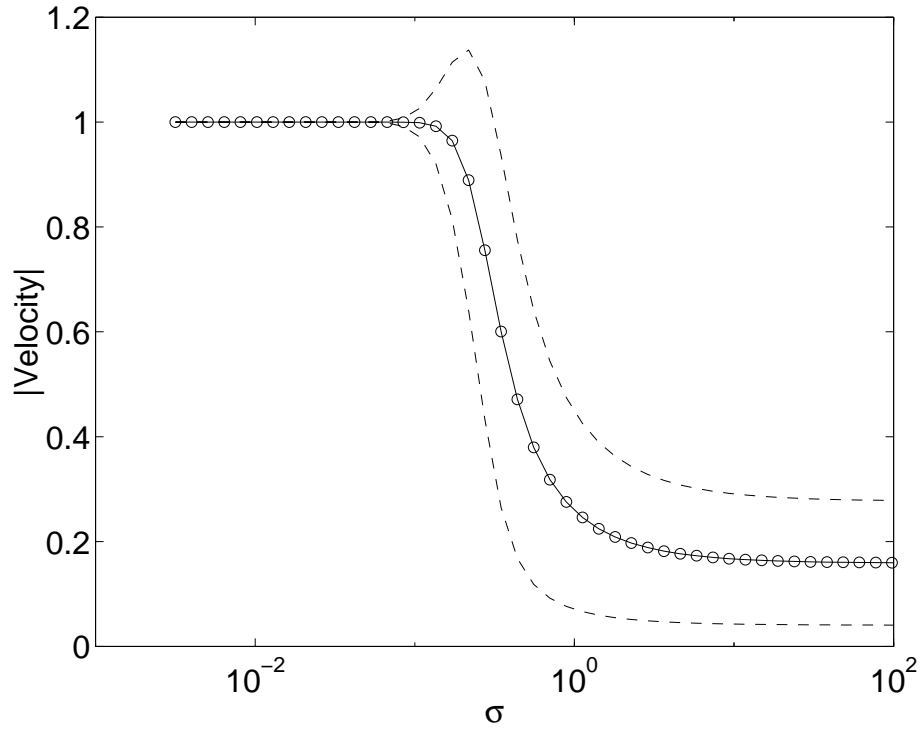
Fig. 7. Absolute value of velocity, $\langle |x(t)| \rangle /t$, from (17), (*circles*), and this quantity plus and minus its standard deviation, from (17) and (18), (*dashed*), as function of noise intensity. β is given by $\beta = e^{-1/\sigma}$, $t = 50$ and $v = 1$